Characterization of the Orientation Parameters Around Crack Tips in Unfilled and Nanofilled Poly(propylene) Using in-situ Synchrotron Small and Wide Angle Scanning Scattering Techniques

Michael Feuchter,[*1,2] *Günther Maier,*[3,4] *Ivo Zizak,*[5] *Gerald Pinter,*[1] *Milan Kracalik,*[6] *Stephan Laske,*[6] *Günter Rüdiger Langecker*[6]

Summary: The fracturing behavior of polymers and polymeric composites is of great interest in the scientific and application community. Especially in the case of silicate-layered nanocomposites the influence of fillers on the fracturing behavior is still fairly unclear. Fractures of semicrystalline polymers are accompanied by various processes of which shearing and cavitations are the most common ones. Nanocomposite deformation due to the delamination of fillers seems to be the most practical way leading to fractures with relatively low strains. With the method of scanning small angle X-ray scattering (SAXS) and wide angle X-ray diffraction (WAXD) it is possible to combine information on the structural details with the position on the sample, with the actual position resolution of the investigation being defined by the size of the X-ray beam used to scan the sample. By means of the application of synchrotron radiation it is nowadays possible to adjust the actual beam size to the dimensions of the region of interest, which is why it is an adequate tool for studying the deformation region near a crack tip. In a native polypropylene sample, the fracturing process was accompanied by shear yielding as well as lamellae fragmentation and reorienting. In the highly deformed material near the crack tip fibrillated material could be found. However, in the polymeric nanocomposites (PNC) shearing, lamellae fragmentation, and fibrillation were hindered by the filler due to which the material did not have so much freedom to dissipate energy and fractures occurred much earlier. In this paper the comparison of a PNC and its native polymer is to provide an overview of the different deformation mechanism and the structural details around the crack tip.

Keywords: crack tip; nanocomposites; orientation; synchrotron radiation; X-ray

Introduction

Polymeric nanocomposites, especially with the filler montmorrillonite, have become of predominant interest to the scientific and application community in the last years [1–4] as the fracturing behavior of polymeric nanocomposites and especially the changes caused by the presence of nanofillers are still rather unclear. For this reason in-situ synchrotron small and wide angle scattering techniques during tensile testing used to be employed to characterize fracturing

[1] Institute of Materials Science and Testing of Plastics, University of Leoben, Franz Josef Strasse 18, 8700 Leoben, Austria
E-mail: Michael.Feuchter@mu-leoben.at
[2] Polymer Competence Center Leoben GmbH, Roseggerstrasse 12, 8700 Leoben, Austria
[3] Erich Schmid Institute and Department of Material Physics, Jahnstrasse 12, 8700 Leoben, Austria
[4] Materials Center Leoben Forschung GmbH., Roseggerstrasse 12, 8700 Leoben, Austria
[5] Berliner Elektronenspeicherring-Gesellschaft für Synchrotronstrahlung m.b.H., Albert-Einstein-Straße 15, 12489 Berlin, Germany
[6] Institute of Plastics Processing, University of Leoben, Franz Josef Strasse 18, 8700 Leoben, Austria

processes under dynamical conditions.[5–9] Another possibility to study fracturing behavior of polymers and their nanocomposites by using synchrotron radiation is scanning around a loaded crack tip and thereby interpreting the texture.[10–14] With this method it is possible to determine the microstructural characteristics around defects and crack tips. Nanoclay fillers can be distributed in the polymer in three different ways: first there are agglomerates of the silicate platelets with overall dimensions in the μm range and no or less interactions between the polymer and the filler. The second state is the intercalated one, in which polymer chains are inclined between two silicate platelets. The interlayer distance increases, but the layers are still stacked. The third state is the exfoliated state with single platelets being randomly distributed in the polymer without any special correlation between each other.[1]

There are different methods to produce polymer nanocomposites.[2] In this study melt compounding has been applied in order to produce intercalated silicate polypropylene nanocomposites since their intercalated structure is of special interest due to its melt compounding process. On the one hand it is always possible that in this process the degree of exfoliation can be less than a hundred percent and that some stacks of intercalated clay can be found in the composite. On the other hand the intercalated structure is a ''natural'' structure (e.g. bone [15–16]) and thus the desired one for (e.g. [17]) for various applications.

Experimental Part

Materials

The isotactic polypropylene (PP) homopolymer HC600TF (MFI 2.8 g/10 min; 230 °C/2.16 kg) has been provided by Borealis Inc., Linz, Austria. As a nanofiller an organically modified montmorrillonite with the commercial indication Nanofil 5, provided by Süd-Chemie Inc., Munich, Germany, has been used. In order to combine the hydrophobic polymer and the hydrophilic nanofiller, a compatibilizer was needed. In this case, the maleinic anhydride acid grafted polypropylene Scona TPPP 2112 FA, provided by Kometra Ltd., Schkopau, Germany, has been chosen.

Sample Preparation

For the compounding process, an intermeshing, co-rotating twin screw extruder Theyson TSK30/40D (Theyson Ltd., Vienna, Austria) with a string die was used. The feed rate was set at 20 kg/h with a screw speed of 150 rpm in the masterbatch sample. First a masterbatch with 20 wt. % nanofiller and 20 wt. % compatibilizer was produced which then was diluted with pure PP down to 5 wt. % nanoclay content.[18–19]

For the structural characterization around crack tips, samples had to prepared by carrying out the following steps: first the granulated materials were pressed to plates with a thickness of 1 mm using a hydraulic vacuum press machine (Collin 200 PV, Dr. Collin Ltd., Ebersberg, Germany). Then rectangular pieces (50×10 mm^2) were cut out of these plates. For the localization of the crack tip and the scanning regions the samples were equipped with a 1 mm deep notch. To do so, the same tool was used as for the production of the charpy test samples. This notch was made on both sides at the middle of the sample's length. In Figure 1 the dimensions of a specimen are indicated.

Scanning SAXS/WAXS

The synchrotron experiments were performed by means of a μ-spot beam line at the BESSY (Berliner Elektronenspeicherring-Gesellschaft für Synchrotronstrahlung m.b.H., Berlin, Germany). This system was equipped with a two-dimensional X-ray detector (Mar Mosaique, Mar Research, Germany). The applied forces were created with the help of a computer controlled tensile testing apparatus (Anton Paar, Graz, Austria). The distance from the sample to the detector was 430 mm, and the wavelength for the experiments was 0.0827 nm. The samples were measured in transmission

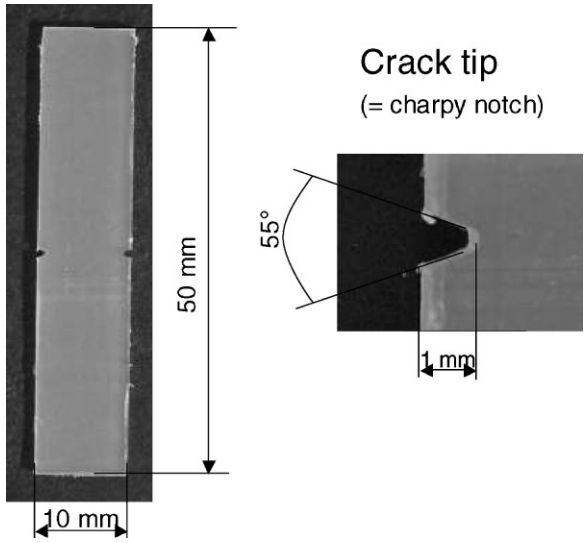

Figure 1.
Illustration of a double notched scanning specimen. On the right side the crack tip is illustrated.

with the size of the last beam definition pinhole having a diameter of 30 μm. Thus, it was possible to measure small angle x-ray scattering (SAXS) and wide angle x-ray diffraction (WAXD) simultaneously.

Mechanical Testing

Figure 2 shows a typical force displacement curve for the selected polypropylene. The samples were stressed with the maximal load, and the scanning experiment was started. The force lost during the scanning experiment due to creep was less than 10%.

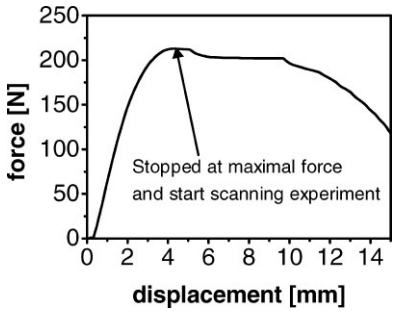

Figure 2.
A typical force displacement curve of polypropylene. The scanning experiment was started at the maximum reached force at which the tensile test machine stopped as well.

Data Evaluation

For the determination of the orientation (= texture) parameters, two-dimensional SAXS data were averaged in azimuthal direction using the Fit2D software.[20] In order to evaluate the data, all scattering curves were corrected for background scatter. Figure 3 shows a typical diffraction pattern recorded near the crack tip. The exact determination of the orientation parameters, such as the direction of the orientation and its degree, of the diffraction pattern in Figure 3 is illustrated in figure 4. The degree of orientation α was calculated by using Equation 1, in which I_p and I_u represent the areas as defined in the diagram on the left in Figure 4. The position of the peaks in the azimuthal intensity distribution (as shown in the diagram on the right side in Figure 4) provided information on the direction of the orientation, and were located by fitting data with a Gaussian function. The WAXD signal, providing information on the crystallographic structure and texture, was only used to gather qualitative information on structural details.

$$\alpha = \frac{I_p}{I_p + I_u} * 100\% \quad (1)$$

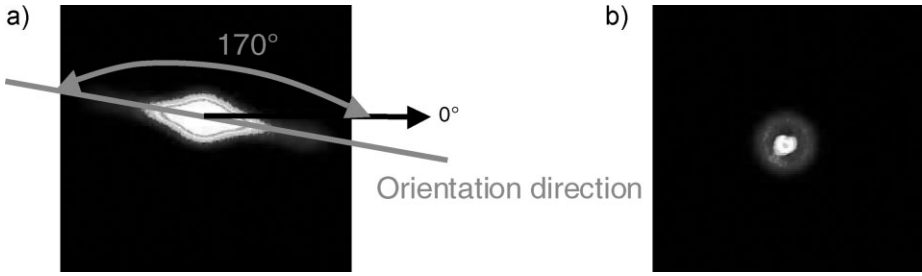

Figure 3.
SAXS diffraction patterns of a high oriented (a) and an isotropic location (b).

Results

For the X-ray scanning experiment special regions of interest were selected. The regions should be near the crack tip in order to find out more about the mechanism at work during the deformation process. The selected regions of interest are illustrated in Figure 5.

Figure 6 and 7 show two-dimensional SAXS and WAXS data. Every visible point or ring demonstrates a single measurement, which means that there are more than 900 diffraction patterns illustrated in each figure. The crack tip could be identified by the black zone in which there was no material. In these two figures the difference between polypropylene and its polymeric nanocomposite can already be recognized. For the quantification of the varieties in the deformation process the orientation parameters can be drawn on.

Near the crack tips, regions with high oriented material could be found in both materials. In virgin polypropylene, microfibrils had been formed as indicated by fiber-like SAXS and WAXD pattern as shown in Figure 8. The corresponding WAXS data from the same measuring point is illustrated on the left side in this figure. Next to the crack tip, the originally isotropic structure changed to a fiber-like structure, where the 110 plane was found to be orthogonal to the fibril direction. The left side in Figure 9 illustrates two-dimensional WAXS data from the nanocomposite. Scattering experiments indicated that the changes in the texture were not as pronounced as in pure PP. The corresponding SAXS data pointed to the formation of microfibrils in the polymeric component. Stacks of intercalated clay has been reoriented in the same direction as the polymeric fibrils.

The degree of orientation around the crack tip, as calculated on the basis of the SAXS data, is illustrated in Figure 10. Figure 10a shows the polymeric nanocom-

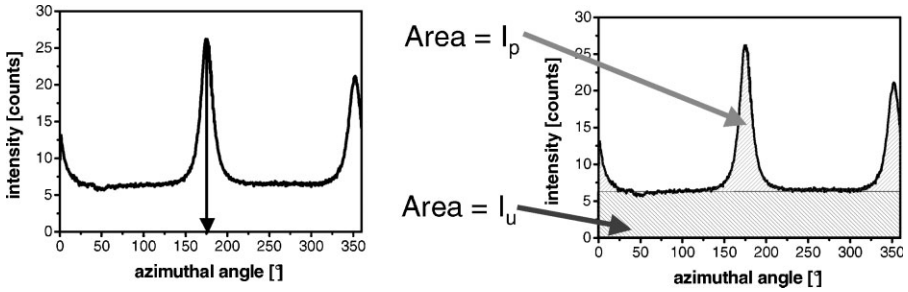

Figure 4.
Determination of orientation parameters. The diagram on the left shows the determination of the orientation direction, while the diagram on the right illustrates the analysis of the degree of the orientation.

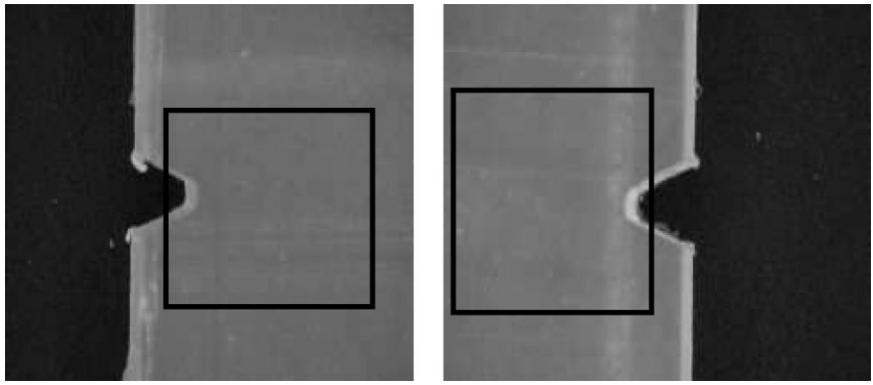

Figure 5.
Regions of interest for the scanning experiment. On the left side the polymeric nanocomposite can be seen. In the picture on the right side the polypropylene is illustrated.

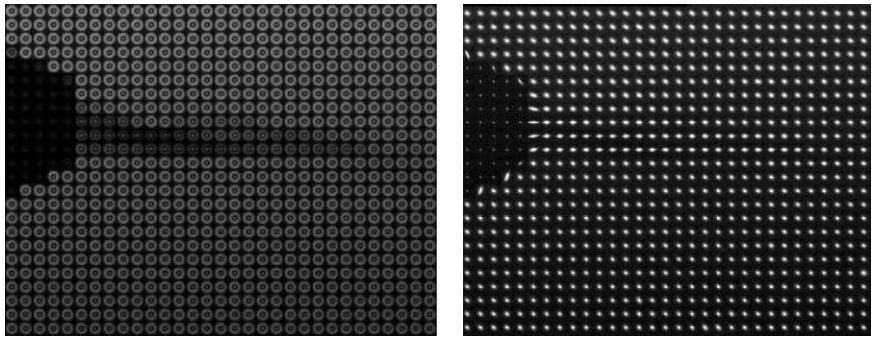

Figure 6.
WAXS data (diagram on the left) and SAXS data (diagram on the right) for PNC.

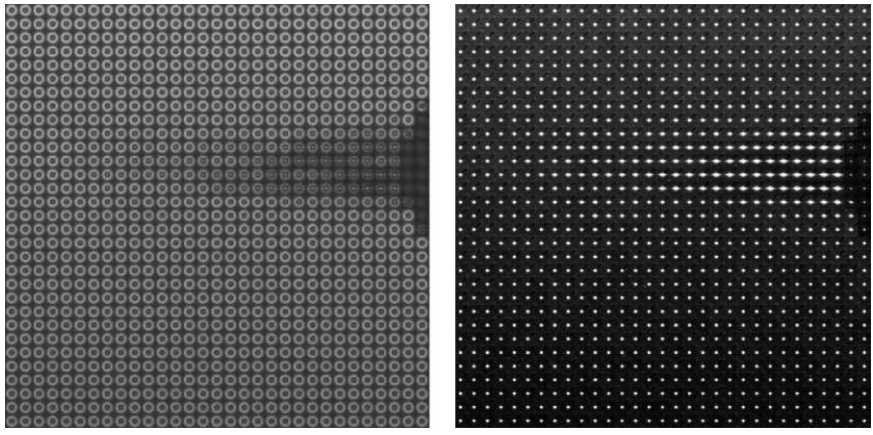

Figure 7.
WAXS data (diagram on the left) and SAXS data (diagram on the right) for polypropylene.

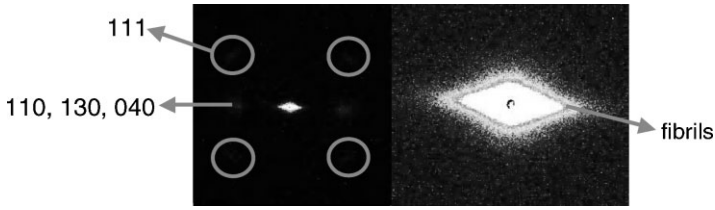

Figure 8.
High oriented WAXS (on the left) and SAXS diffraction pattern of polypropylene.

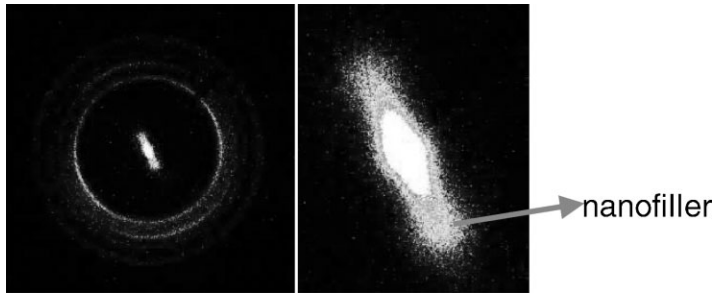

Figure 9.
High oriented WAXS (on the left) and SAXS diffraction pattern of PNC.

posite, while in Figure 10b the orientation of the virgin polypropylene can be seen. The main difference between these two materials could be determined in the characteristics of the oriented zone. In polymeric nanocomposites there was a very thin but high oriented region almost over the entire measuring region, while in virgin polymer a broader and shorter zone could be found.

The direction of the microfibrils and of the stacks of intercalated clay around the crack tip are shown in Figure 11a and b. It can be seen that the direction of the high oriented fibrils changed around the tip. The intercalated filler likewise more or less followed the orientation of polymer which implies that stacks of filler rotated to follow the main shear stress direction equal to the polymer. This effect may have been caused

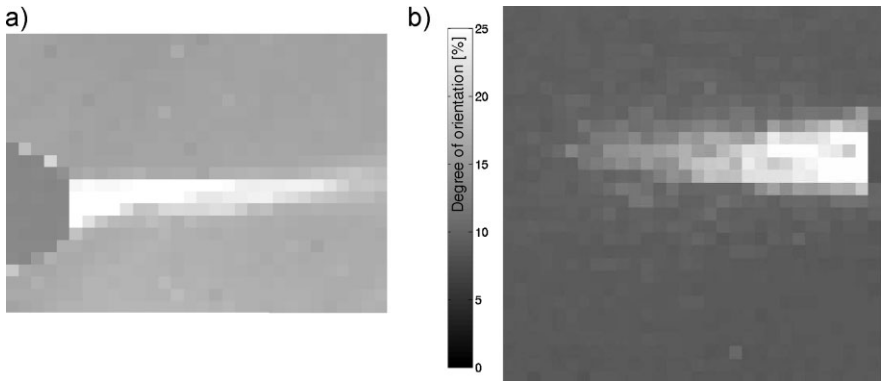

Figure 10.
Degree of orientation. In Figure 10a a scan of the polymeric nanocomposite is shown, and in figure 10b a scan of the polypropylene can be seen.

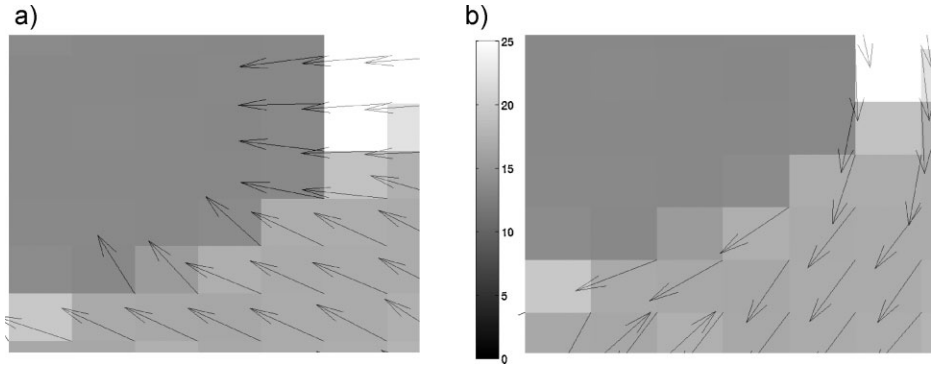

Figure 11.
Direction of the stacked nanofiller (a) and the generated microfibrils (b) around the crack tip.

by stress distribution around a defect. However, the same characteristics, yet more pronounced, were found in polypropylene as well.

Discussion

Around the crack tips the originally isotropic material changed to an oriented, fiber-like structure. These fibrils follow the main shear stress directions in the polymer which is an effect that can especially be seen in the SAXS pattern. The orientation and the degree of the orientation of the microfibrils clearly indicate the effects in the material. In nanocomposites the stacked nanofiller is perpendicularly oriented to the microfibrils which indicates that stacks are arranged around the formed fibrils. Due to the high aspect ratio of the stacked nanoclay (10–20 layers per stack), the highest free surface of the stacks would be on the top (and the bottom) of the thereby formed cylinder. These stacks would be arranged in such a way that the free surface could interact with the free surface of the microfibrils.

In pure PP samples, the WAXD pattern also indicates the formation of a fiber-like orientation next to the crack tip. However, this phenomenon could not be observed in polymeric nanocomposites. Deformation processes are therefore different in PP and clay-PP composites. In pure PP shearing, lamellae rotation, and the complete reorientation of the crystalline lattice are possible, while the nanofiller reduces the freedom. As shear bands, originating from highly deformed areas, could not develop, smaller plastic zones and stress concentration in nanocomposites were the result. This can be seen in Figure 10, in which the orientation parameters of both types of samples are shown. Therefore, fractures occur at significantly lower strains compared to pure PP.

Conclusion

The fracture properties of polypropylene or its nanocomposite strongly depend on the degrees of freedom in the material to react to external forces. The formation of plastic zones, accompanied by a reorientation of the crystalline lattice, and of microfibrils can be imaged by scanning SAXS and WAXS. An orientation parameter to quantify the dimensions and the structure of plastic zones has been used. The pure polymer featured a very broad orientation zone allowing the material to yield. Therefore, the dominant material behavior was ductile. However, the nanocomposite has shown different formations of the high oriented region (= plastic zone). The rather thin, high oriented plastic zone with ran from one crack tip to the opposite ones. In contrast, no strong reorientation of the

crystalline lattice has occurred in the PP sample as one of the main stress relaxation mechanisms of the polymer has been hindered by the filler. Since the stress concentrated in the polymer part of the composite, the plastic zone formed between the two notches and the material showed a dominant brittle material behavior.

Acknowledgements: The research work of this paper was performed within the Research Project Cluster NanoComp (''Performance Optimization of Polymer NanoComposites''), coordinated by the Polymer Competence Center Leoben GmbH. Funding by the Federal Ministry of Traffic, Innovation and Technology and the Austrian Research Promotion Agency within the AUSTRIAN NANO-Initiative is gratefully acknowledged. The help during the synchrotron experiments at the μ-spot beam line (BESSY, Berlin, Germany) by Dr. Ivo Zizak and Prof. Dr. Oskar Paris is highly appreciated. This work was supported by the European Community – Research Infrastructure Action under the FP6 ''Structuring the European Research Area'' Program (through the Integrated Infrastructure Initiative ''Integrating Activity on Synchroton and Free Electron Laser Science'' – Contract R II 3-CT-2004-506008).

[1] S. S. Ray, M. Okamoto, *Prog. Polym. Sci.* **2003**, *28*, 1539.
[2] M. Alexandre, P. Dubois, *Materials Science and Engineering* **2000**, *28*, 1.
[3] S. C. Tjong, *Materials Science and Engineering R* **2006**, *53*, 73.
[4] S. Pavlidou, C. D. Papaspyrides, *Progress in Polymer Science* **2008**, *33*, 1119–1198.
[5] N. Stribeck, U. Nöchel, S. S. Funari, T. Schubert, A. Timmann, *Macromol. Chem. Phys.* **2008**, *209*, 1992–2002.
[6] M. C. Garcia Gutierrez, J. Karger-Kocsis, C. Riekel, *Chemical Physics Letters.* **2004**, *398*, 6–10.
[7] C. Lorenz-Haas, P. Müller-Buschbaum, T. Ittner, J. Kraus, B. Mahltig, S. Cunis, G. V. Krosigk, R. Gehrke, C. Creton, M. Stamm, *Phys. Chem. Chem. Phys.* **2003**, *5*, 1235–1241.
[8] C. Lorenz-Haas, P. Müller-Buschbaum, O. Wunnicke, C. Cassignol, M. Burghammer, C. Riekel, M. Stamm, *Langmuir* **2003**, *19*, 3056–3061.
[9] R. J. Davies, N. E. Zafeiropoulos, K. Schneider, S. V. Roth, M. Burghammer, C. Riekel, J. C. Kotek, M. Stamm, *Colloid Polym Sci.* **2004**, *282*, 854–866.
[10] G. A. Maier, G. Wallner, R. W. Lang, P. Fratzl, *Macromolecules* **2005**, *38*, 6099–6105.
[11] G. A. Maier, G. M. Wallner, R. W. Lang, J. Keckes, H. Amenitsch, P. Fratzl, *J. Appl. Cryst.* **2007**, *40*, 564–567.
[12] N. E. Zafeiropoulos, R. J. Davies, S. V. Roth, M. Burghammer, K. Schneider, C. Riekel, M. Stamm, *Macromol. Rapid Commun.* **2005**, *26*, 1547–1551.
[13] A. Boger, B. Heise, C. Troll, O. Marti, B. Rieger, *European Polymer Journal* **2007**, *43*, 3573–3586.
[14] F. Heidelbach, C. Riekel, H.-R. Wenk, *J. of Appl. Crys.* **1999**, 32, 841–849.
[15] P. Fratzl, R. Weinkamer, *Progress in Materials Science* **2007**, *52*, 1263–1334.
[16] P. Fratzl, H. S. Gupta, O. Paris, A. Valenta, P. Roschger, K. Klaushofer, *Progr Colloid Polym Sci.* **2005**, *130*, 33–39.
[17] P. Podsiadlo, A. K. Kaushik, E. M. Arruda, A. M. Waas, B. S. Shim, J. Xu, H. Nandivada, B. G. Pumplin, J. Lahann, A. Ramamoorthy, N. A. Kotov,1 *SCIENCE 318*, 80–83.
[18] S. Laske, M. Kracalik, M. Gschweitl, M. Feuchter, G. Maier, G. Pinter, R. Thomann, W. Friesenbichler, G. R. Langecker, *Journal of Applied Polymer Science* **2009**, *111*, 2253–2259.
[19] S. Laske, M. Kracalik, M. Gschweitl, M. Feuchter, G. Maier, G. Pinter, R. Thomann, W. Friesenbichler, G. R. Langecker, *Journal of Applied Polymer Science* **2009**, in press.
[20] A. P. Hammersley, S. O. Svensson, M. Hanfland, A. N. Fitch, D. Hausermann, *High Pressure Research* **1996**, *14*, 235–248.

